J Solid State Electrochem (2001) 5: 94–106

ORIGINAL PAPER

Essadik Abdeljalil · Bineta Keita · Louis Nadjo
Roland Contant

STM and AFM characterization of thin metal oxide films electrodeposited from $[P_2Mo_{18}O_{62}]^{6-}$

Received: 4 January 2000 / Accepted: 15 February 2000

Abstract Two groups of techniques have been devised for the electrodeposition of new electroactive oxide films from $[P_2Mo_{18}O_{62}]^{6-}$. In the first group, two adsorption procedures were used: simple immersion of the electrode in a solution containing 10^{-4} M $[P_2Mo_{18}O_{62}]^{6-}$ in a pH 3.50 medium or cycling of the electrode in this solution in the potential domain of the first three two-electron waves of the heteropolyanion results in surfaces which retain the oxometalate by mere adsorption. Strikingly, during the cycling, it was found that a fourth wave appears in the potential domain of the first three two-electron waves of $[P_2Mo_{18}O_{62}]^{6-}$, indicating an evolution of the heteropolyanion in the solution. Such an evolution was also observed with aged solutions. Then, the potential program for the actual modification step was run by cycling either of these electrodes from −0.2 V to −0.87 V vs. SCE in pure supporting electrolyte. Analysis of the STM images of the surfaces show essentially monomers 1.2–1.5 nm in diameter just after adsorption and a sizeable increase of the dimensions of the patterns after modification. The predominant sizes of these aggregates after modification remain in the range 10–12 nm. The second group of techniques consists in a modification of the electrode surface directly in the solution containing the heteropolyanion. A fixed potential as well as cycling prove efficient. Thick films are obtained readily, which are better imaged by tapping mode AFM. An increase of the pH to 4.50, in appropriate conditions, seems to be favourable to the deposition kinetics. The aggregates in the topmost layers are up to 40 nm in diameter and are assembled in interconnected islands. As a whole, these two groups of techniques appear to exert an important influence on the aggregate sizes. The paper demonstrates that these sizes might be relatively well controlled by the choice of experimental conditions.

Key words Heteropolyanion · Oxide film · Chemically modified electrodes · Scanning tunnelling microscopy · Cyclic voltammetry

E. Abdeljalil · B. Keita · L. Nadjo (✉)
Laboratoire de Physicochimie des Rayonnements,
UMR 8610, CNRS, Electrochimie et Photoélectrochimie,
Université Paris-Sud, Bâtiment 420,
91405 Orsay Cedex, France
e-mail: nadjo@icmo.u-psud.fr
Tel.: +33-1-69157751; Fax: +33-1-69154328

R. Contant
Laboratoire de Chimie des Métaux de Transition,
UPRESA 7071, CNRS, Université Paris VI,
4 Place Jussieu, 75252 Paris Cedex 05, France

Supplementary material:
Additional documentary material has been deposited in electronic form and can be obtained from http://link.springer.de/link/service/journals/10008/index.htm

Introduction

A constant line in our aims during the study of oxometalates is the possibility to transfer to electrode surfaces their known catalytic properties towards numerous chemicals in solution. The idea behind this effort is to take advantage of the now well-established usefulness of (W^{VI}, W^{V}) or (Mo^{VI}, Mo^{V}) mixtures as good catalysts and electrocatalysts [1–5]. In recent papers, we have demonstrated that new electroactive metal oxides can be electrodeposited from heteropolyanions [6, 7] in relatively mild conditions. The focus was placed essentially on the study of $[P_2Mo_{18}O_{62}]^{6-}$, which is one of the representative heteropolyanions in the catalytic and quantitative reduction of NO to N_2O [8]. Adherent, persistent and electrochemically active films were obtained by potential cycling. It has been possible to cycle the same sample several hundred times in a plain supporting electrolyte, without observing any tendency to dissolution. Among interesting behaviour revealed by an electrochemical quartz crystal microbalance (EQCM) study, it is worth emphasizing a steady current increase and mass increase of the freshly deposited films during their continuous cycling in the pure supporting electrolyte. This

observation was rationalized by considering the swelling of the films by continuous water and electrolyte uptake during their redox processes up to a maximum, after which only intercalation/deintercalation processes are operative. Close analogy with the behaviour of WO_3 and MoO_3 bronzes was stressed as well as the remarkable aforementioned stability of the present films.

The wealth and variety of the observed behaviour demand that complementary work, in several directions, be performed for a better understanding of these films. In this context, the present paper is devoted to the electrochemistry, scanning tunnelling microscopy (STM) and atomic force microscopy (AFM) study of films electrodeposited from $[P_2Mo_{18}O_{62}]^{6-}$, with particular emphasis on the early stages of the deposition and/or on thin films, in an attempt to find out the main experimental parameters that control the sizes of the agglomerates.

Experimental

Chemicals

Pure water from a Milli-RO_4 unit followed by a Millipore Q purification set was used throughout. All the chemicals were of high-purity grade and were used as received. H_2SO_4, Na_2SO_4 (Prolabo) and CF_3CO_2H, CF_3CO_2Na (Aldrich) were commercial products. Except for one example in which a CF_3CO_2H/CF_3CO_2Na mixture was used, the electrolyte was made up with 0.5 M Na_2SO_4 + H_2SO_4. The pH 3.50 and 4.50 media used in this work were ajusted to these figures by appropriate addition of H_2SO_4 or NaOH, respectively. The preparation and characterization of $[P_2Mo_{18}O_{62}]^{6-}$ (abbreviated as P_2Mo_{18}, in the following) have been described previously by one of us [9]. In the present case of P_2Mo_{18}, the experiment was started, when necessary, with the two-electron reduced species. As a matter of fact, this heteropolyanion is not stable at pH 4.50 but its two-electron reduced species is stable [10, 11]. Starting from this reduced species for our experiments has no deleterious consequences as the new films are known to build up beyond the third two-electron wave of P_2Mo_{18}. Therefore, the heteropolyanion is thoroughly reduced with 2 F/mol in a pH 3.50 medium, and then the pH was adjusted to 4.50 for subsequent work.

The solutions were deaerated thoroughly for at least 1 h with pure argon and kept under a positive pressure of this gas during the experiments.

Apparatus and electrochemical set-up

The reference electrode was a saturated calomel electrode (SCE), the counter electrode a platinum gauze of large surface area. These electrodes were kept in compartments containing the appropriate supporting electrolyte and separated from the working electrode compartment by a medium-porosity glass frit for the counter electrode and a fine-porosity ceramic frit for the reference electrode. The working electrode was either a glassy carbon disc (GC, Tokai, Japan, or Le Carbone Lorraine, France) or a freshly cleaved HOPG surface (Le Carbone Lorraine, France). The mounting and polishing of the glassy carbon have been described previously along with a home-made electrochemical set-up [12]. The glassy carbon samples had a diameter of 3 mm. The electrochemical set-up was either the one described previously with a Sefram TGM 164 XY recorder or an EG&G 273A driven by a PC with the 270 software. In the latter case, the data were recorded in the computer and then printed, when necessary, on a HP DeskJet 560C printer. Experiments were performed at the laboratory temperature.

Microscopy

The STM and most AFM observations were carried out in air at atmospheric pressure. STM experiments were performed with a Molecular Imaging microscope, driven by a Nanoscope III controller (Digital Instruments, Santa Barbara, Calif.). For STM, Pt/Ir wires (80/20) were employed as tunnelling tips. As usual, their quality was checked by imaging a bare freshly cleaved HOPG surface with atomic resolution. High-quality raw data were obtained and are shown hereafter in the current mode. For AFM, the Nanoscope III and its microscope were used. In situ AFM experiments were performed in the contact mode with the EG&G 273A as an external potentiostat. For the ex situ imaging, the Nanoscope III was equipped with an extender electronics module. The images were acquired exclusively in the tapping mode, using a silicon cantilever. This most popular oscillatory AFM technique is particularly suited for the imaging of delicate samples. Two different data types can be collected. Deflection data describe the change in the amplitude directly. Height data correspond to the change in piezo height needed to keep the vibrational amplitude of the cantilever constant.

The extender electronics module offers new possibilities to the tapping mode AFM. It improves the results by providing phase and frequency detection capabilities. In addition, the phase and frequency signals are claimed to be generally immune to interferences and artifacts.

We have been also interested in phase imaging. Recently, we have used this technique to discriminate between metal clusters and the surfactant polymer [13]. Phase imaging has also been illustrated on several hard and soft samples in a paper that emphasizes different useful experimental aspects of the technique [14]. Phase images are shown in the present work only in cases where they appear largely sharper than height-mode images. Dimension measurements were usually performed on images recorded in the height mode. The XY ranges for the scanners were 10 μm for STM and 18 μm for AFM.The scan rates for image acquisition are indicated in the appropriate captions.

In STM as well as in AFM, very good quality raw data were obtained and no filtering was applied to the images.

Results and discussion

The main guidelines, which were helpful to devise the experimental procedures, deserve emphasis. The first one concerns the adsorption behaviour of oxometalates. Owing to their numerous catalytic properties, the adsorbability of heteropoly- and isopolyanions on various materials has been studied by a variety of techniques [15–20 and references therein]. In particular, the oxidized form of heteropolyanions has been demonstrated previously [21, 22] by EQCM to adsorb on electrode surfaces. A second guideline, learnt from our previous work [6, 7], indicates that in order to obtain an adherent and persistent film, six or more electrons/molecule must be fixed on the framework of P_2Mo_{18}. The electrochemistry of P_2Mo_{18} has been described [6, 9–11]. In the pH domain where the anion is stable (pH < 4) [22], each of its first three waves features a two-electron reversible system. The electrodeposition sequences, which will be described, take these remarks into account. In these sequences, the actual modification process, which

we will refer to as "modification", consists in cycling or poising the electrode potential in a domain negative of the third two-electron wave of P_2Mo_{18}. Several independent replications were carried out for each experiment and prove reproducible. The most characteristic film behaviour and morphologies are described hereafter.

Adsorption and modification techniques

Two nuances of adsorption have been developed.

Adsorption by dip coating and modification

Typically, the HOPG electrode was dipped overnight, and up to 24 h, in a pH 3.50 solution containing 10^{-4} M P_2Mo_{18}. It was then taken out, rinsed twice with the supporting electrolyte (0.2 M Na_2SO_4 + H_2SO_4), twice with pure Millipore Q water and left to dry in air before examination by STM. This rinsing procedure will be used throughout for all the experiments in the following. Figure 1 shows a characteristic STM image of the surface after the aforementioned treatments. The coverage of the HOPG surface is apparently dense and relatively uniform. The image in Fig. 1B, which is an enlargement of a domain in Fig. 1A, suggests the presence of individual molecules. These entities have an average diameter of 1.4 nm, even though it clearly appears that these patterns are not actually perfect spheres. As a matter of fact, Dawson-type species are better accommodated in ellipsoids. Nonetheless, the measured dimension would correspond very closely to that expected for P_2Mo_{18} molecules. Detailed examination of the entities in numerous places of several large-scale images of the surface reveals, besides monomers and some larger assemblies, the presence of grains 0.16–0.25 nm in diameter, which might represent sulfate anions and carbon atoms of the HOPG. Such small objects are worth mentioning, because it happens that they do not appear in the size distribution established for Fig. 1A and shown in Fig. 1C. Strikingly, the sizes in Fig. 1C are distributed around two well-separated values: the main one corresponds very closely to the diameter of the P_2Mo_{18} molecule; the second one features larger assemblies around, presumably, dimeric species. The latter pattern might be attributed to decomposition followed by oligomerization/polymerization processes of P_2Mo_{18}. As a matter of fact, lacunary anion fragments are likely to assemble into larger clusters [23]. A possible rationale for this assumption in the present issue comes from the fact that the pH of the supporting electrolyte is at the limit of stability for the heteropolyanion, thus favouring its evolution. Cyclic voltammetry indicates such an evolution for aged P_2Mo_{18} solutions in pH 3.50 medium. Behaviour which can be interpreted in a similar way will also appear in the following with the second electrodeposition procedure.

The preceding electrode is then taken to the deaerated pure supporting electrolyte for modification, accomplished here by cycling between −0.2 V and −0.87 V at a scan rate of 100 mV/s. Exactly the same procedures, except for the STM imaging, were carried out with a 3 mm diameter glassy carbon electrode. The electrochemistry of the two kinds of electrodes was found to be the same during the modification sequence. Figure 2 shows the evolution of the cyclic voltammograms during the cycling of the HOPG electrode. The following main conclusions were culled from all such modifications performed in this work. The cyclic voltammogram starts with modest current intensities and a clear but poorly developed anodic wave. During the first several runs, an induction period is observed with a steady decrease of the cathodic peak current while the associated anodic peak current increases. Finally, a broad reversible and rather symmetrical wave is obtained. During subsequent cycles, the cathodic and anodic currents increase at a relatively fast rate compared to the slow evolution observed during the induction period. The whole pattern remains broad and symmetrical. Such behaviour is observed at the beginning of the modification process. It is also obtained with modified electrodes taken out of the electrolyte and left without polarization for several hours. During the cycling, the cathodic peak potential moves distinctly in the positive direction and the anodic to cathodic peak potential difference remains small. We note, not unexpectedly, that the peak potential location depends on the pH of the supporting electrolyte, but the study of this parameter was not performed further.

The STM image of such a modified surface is illustrated in Fig. 3. In this image, the deposit is thick and relatively uniform. This area was retained because it is the only one among several replications of the same experiment on different HOPG cuts to show in its centre a series of aligned patterns, which, therefore, are believed to follow the defects of the underlying electrode. Enlargement of this area of the surface reveals that discrete agglomerates could be isolated and measured with a diameter ranging roughly from 4 to 11 nm., with most of them in the domain of 6–8 nm. Thus the modification process, whatever its duration, typically up to more than 20 h, favours the agglomeration, but to a limited extent, of the entities present on the surface. It is tempting to ascribe this limitation to the fact that a minute amount of the molecules has been adsorbed on the electrode.

Electrochemical adsorption and modification

Adsorption of the heteropolyanion has been realized by continuous cycling of the glassy carbon or HOPG electrode from +0.60 to −0.32 V in a pH 3.50 solution containing 10^{-4} M P_2Mo_{18}. This potential domain encompasses the first three two-electron waves of the heteropolyanion in this medium. This cycling has been shown previously [6] to result merely in the adsorption of the oxometalate on the electrode surface and not in the

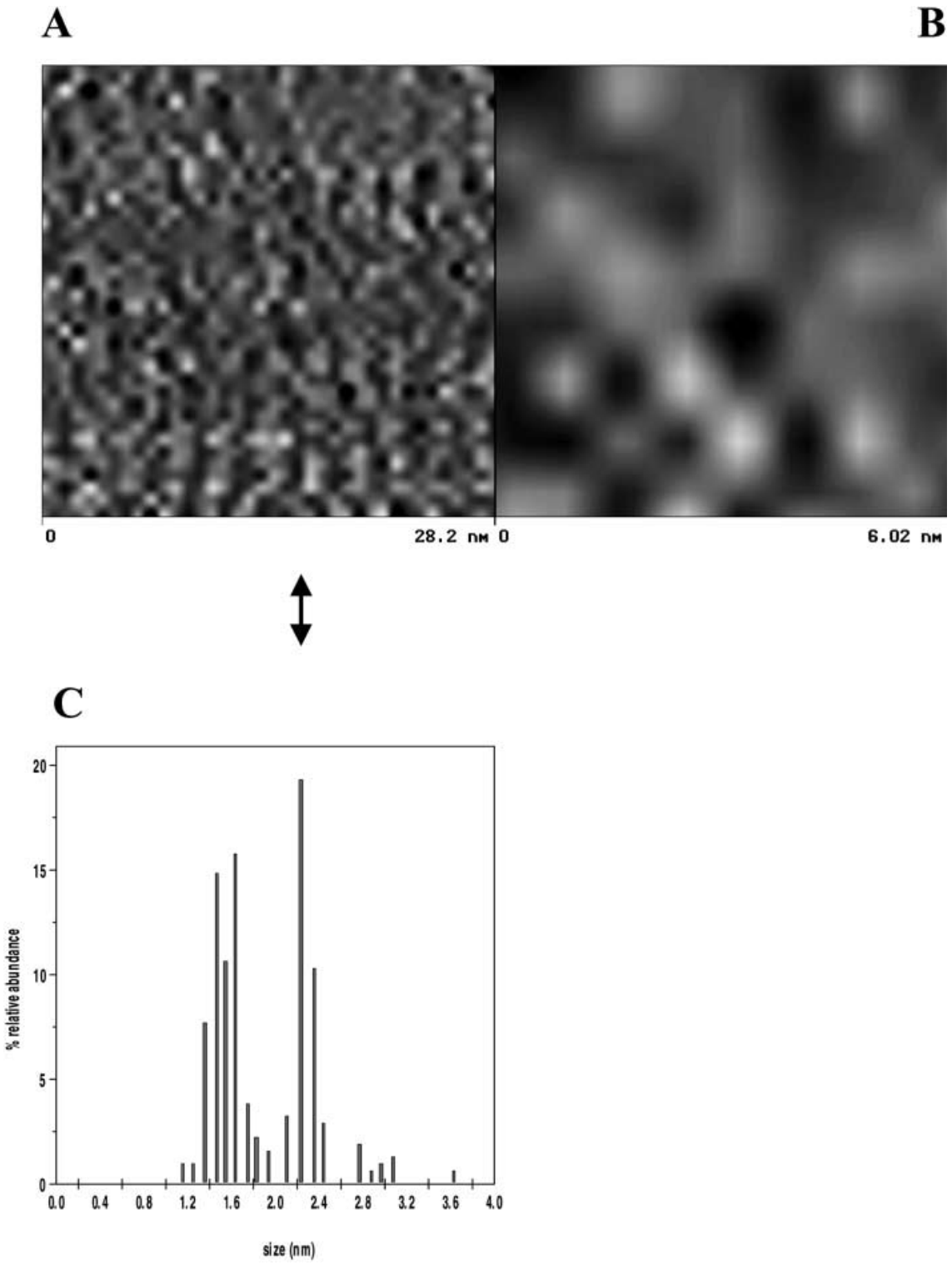

Fig. 1 **A** Current mode STM image of $[P_2Mo_{18}O_{62}]^{6-}$ adsorbed on a HOPG electrode. The surface was obtained by soaking the electrode for 24 h in a solution of 0.2 M Na_2SO_4 + H_2SO_4 (pH 3.50) + 10^{-4} M $[P_2Mo_{18}O_{62}]^{6-}$. Image **B** is an enlargement of image **A**, from which the size of the molecule is easily measured. Image scan rate: 1.40 Hz. No filtering was applied. For further details, see text

modification process. Figure 4 illustrates this adsorption step. Interestingly, after a few runs, a fourth wave appears in the preset potential domain and grows steadily at each other cycle. This wave becomes progressively reversible, and, in the long run, becomes as large as the first three ones. To our knowledge, the evolution of this new wave is clearly described here for the first time.

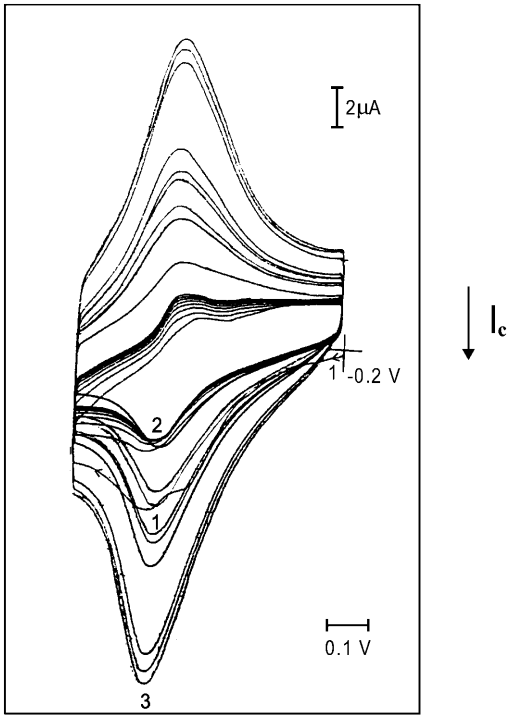

Fig. 2 Evolution of the cyclic voltammograms run with the preceding electrode in pure supporting electrolyte, 0.2 M Na_2SO_4 + H_2SO_4 (pH 3.50), during the modification step between −0.2 V and −0.87 V vs. SCE. The *numbers* on the curves sketch the time evolution of the cathodic current during the modification. For further details, see text

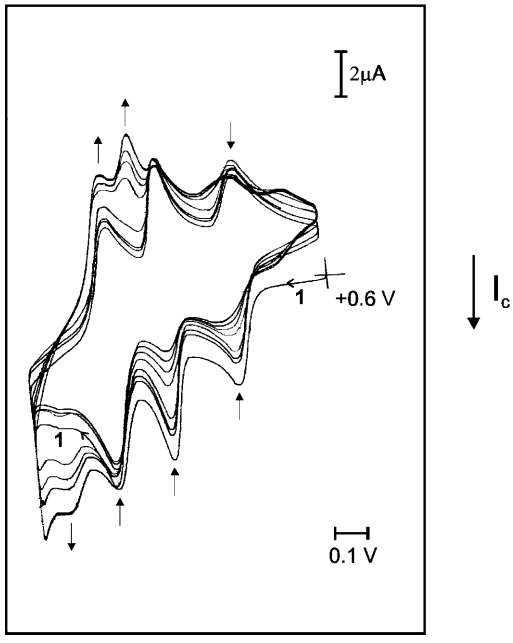

Fig. 4 Evolution of the voltammetric pattern during the continuous cycling of a HOPG electrode between +0.60 V and −0.32 V vs. SCE in a solution of 0.2 M Na_2SO_4 + H_2SO_4 (pH 3.50) + 10^{-4} M $[P_2Mo_{18}O_{62}]^{6-}$. A fourth wave appears and grows gradually in this potential domain. For further details, see text

Fig. 3 **A** Current mode STM image of the electrode of Fig. 2. Image **B** is an enlargement of image **A**. No filtering was applied. Image scan rate: 2.11 Hz. For further details, see text

Figure 5 shows a typical STM image of the surface of a HOPG electrode cycled for 22 h, and then taken out, rinsed and dried. Several striking features are observed. A large-scale image, roughly 250 × 250 nm^2, is shown in Fig. 5A, as an example of a representative pattern of the electrode surface. Figure 5B is an enlarged scale area of Fig. 5A, where the motifs are better visible and from which measurements are possible. However, Fig. 5A itself was preferred as being more representative for a

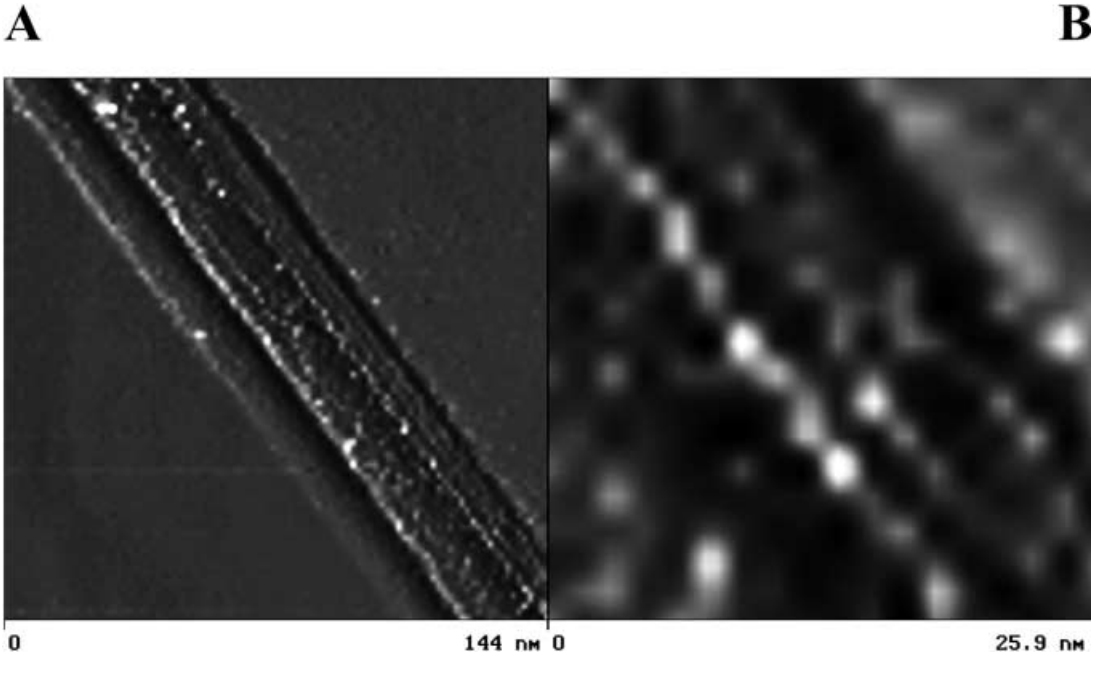

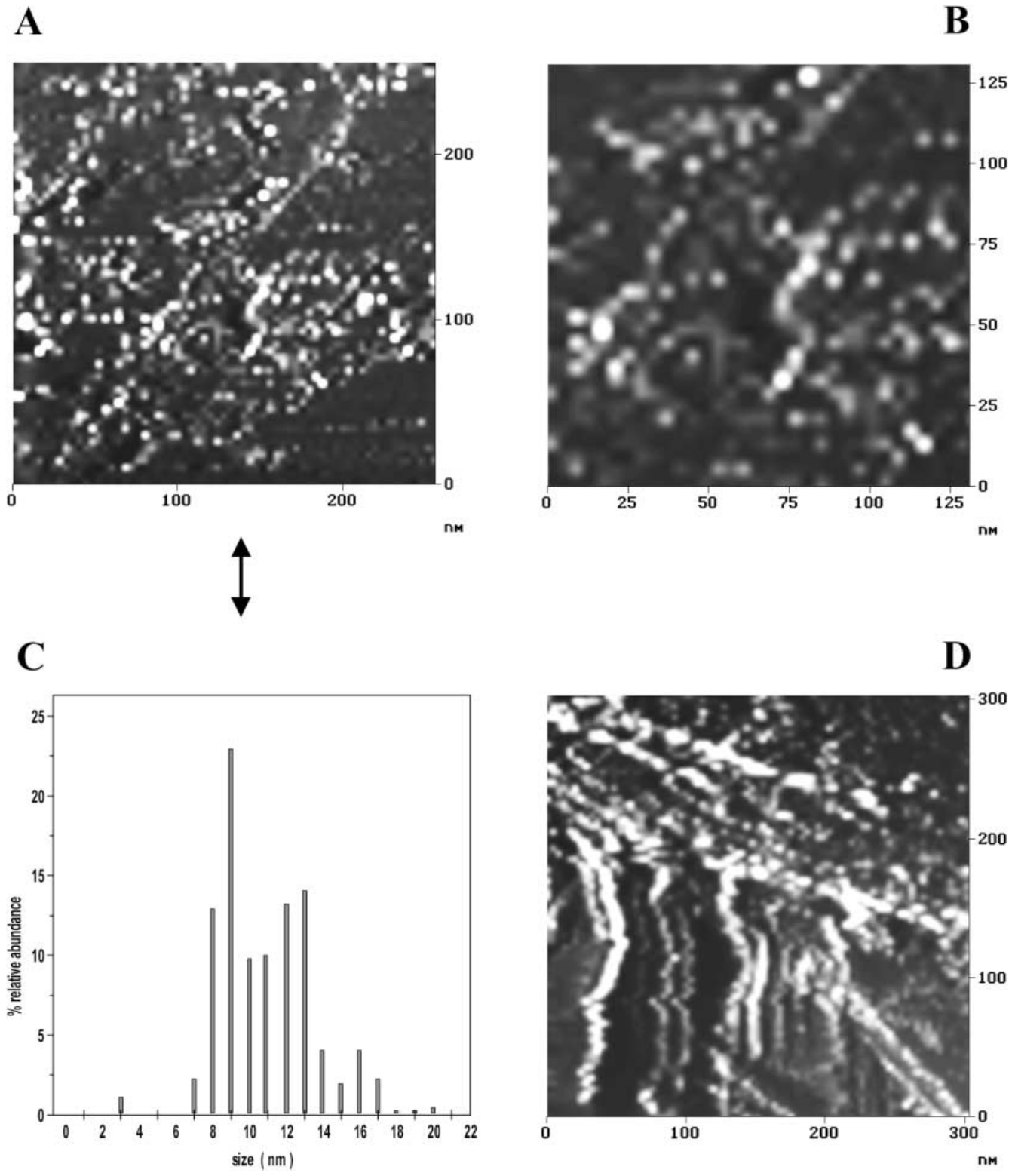

Fig. 5A–D Current mode STM images in two representative domains of a HOPG electrode cycled continuously for 22 h between +0.60 V and −0.32 V vs. SCE in a solution of 0.2 M Na_2SO_4 + H_2SO_4 (pH 3.50) + 10^{-4} M $[P_2Mo_{18}O_{62}]^{6-}$. **A**, **B** a typical domain and its enlargement; **C** size distribution diagram of **A**; **D** a second representative domain. Image scan rate: 1.19 Hz. No filtering was applied. For further details, see text

statistical evaluation of the dimensions of the entities on the surface. Figure 5C shows the distribution of sizes. The agglomerates with a size between 6 and 18 nm are preponderant, with a particular abundance around 8–9 nm. Indeed, monomers are present, but the phenomenon worth mentioning is the appearance of new, larger dimension motifs with a relatively narrow distri-

bution. Comparison of the dimensions from Figs. 1A and 5A shows that the sizes of the agglomerates are slightly different, but not in a proportion that would have made their comparison impossible. This observation suggests a limited variation of aggregate sizes with the adsorption technique. In Fig. 5D, showing another characteristic domain, the patterns are arranged in distorted lines and rows, inside which individual agglomerates are distinguishable. This organization differs from the one observed in Fig. 1A. Tentatively, we ascribe the formation of these aggregates in the representative areas of the surface to the evolution of the heteropolyanion in the pH 3.50 medium. The appearance of a fourth wave in Fig. 4 should be traced to such an evolution. Furthermore, during the electrochemical adsorption, the process of aggregation might be favoured by the presence of reduced molecules in the solution and, thus, explain the increase of sizes.

In another experiment, the electrochemical adsorption procedure was used for 14 h and is then complemented by 5 h modification by cycling in pure supporting electrolyte. Figure 6 has been selected as a typical representative area of the surface showing several levels of relatively flat planes with sharp borders. The vertical distance from one plane to the next in Fig. 6B is in the range 1.2–1.5 nm, indicating monolayer vertical spacing between these planes. Only 1.5 nm distances are marked in Fig. 6B. The average dimension of the entities which constitute rows, ropes and borders which can be seen in Fig. 6A is 4–5 nm. Analogous arrangements of planes are also observed in other experiments, except that monomolecular height steps are not so common.

Fig. 6 **A** Current mode STM image of a HOPG electrode cycled continuously for 14 h between +0.60 V and −0.32 V vs. SCE in a solution of 0.2 M Na_2SO_4 + H_2SO_4 (pH 3.50) + 10^{-4} M $[P_2Mo_{18}O_{62}]^{6-}$ and then submitted to the modification program by cycling for 5 h between −0.2 V and −0.87 V vs. SCE in pure supporting electrolyte. Image scan rate: 1.02 Hz. No filtering was applied. For further details, see text. **B** Section drawn along the line in **A** and showing the monolayer vertical spacing of the planes

Direct modification in the deposition medium

Direct potentiostatic modification in the deposition bath

For this modification technique, the electrode potential was set to −0.800 V in the deposition bath for 5 min. The potential is chosen close to the most negative limit used for the modification by cycling. The duration was found to be appropriate for the build-up of sufficiently thin films which could be studied by STM. Even so, the STM image reveals a relatively dense coverage of the electrode surface. Monomers and smaller objects are clearly identified by their dimensions, along with other entities 5–6 nm in diameter. It is remarkable that the deposition of a thin film by the potentiostatic technique gives patterns which are close in dimension to those obtained in the other procedures, provided the electrolysis time is short enough.

Direct modification by cycling without a preadsorption step

For this purpose, the electrode potential was cycled directly between −0.2 V and −0.82 V in the modification

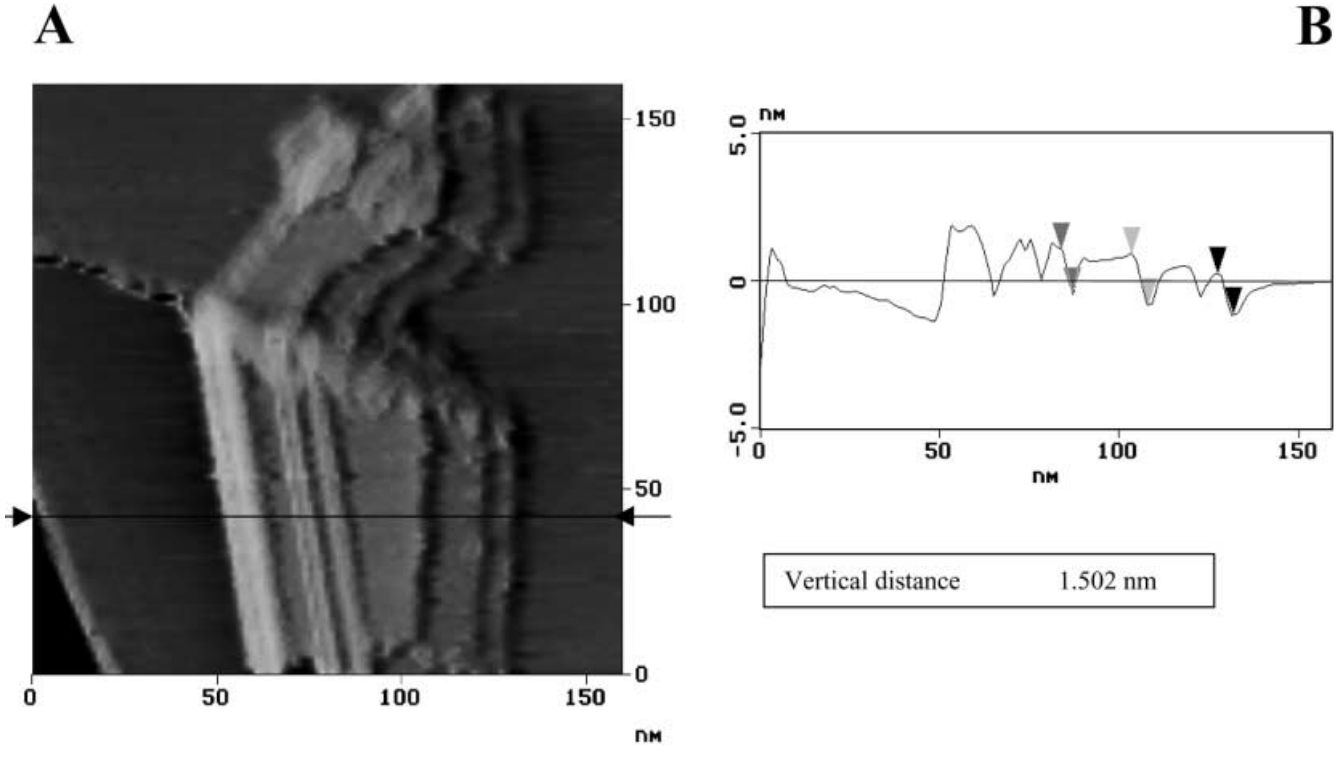

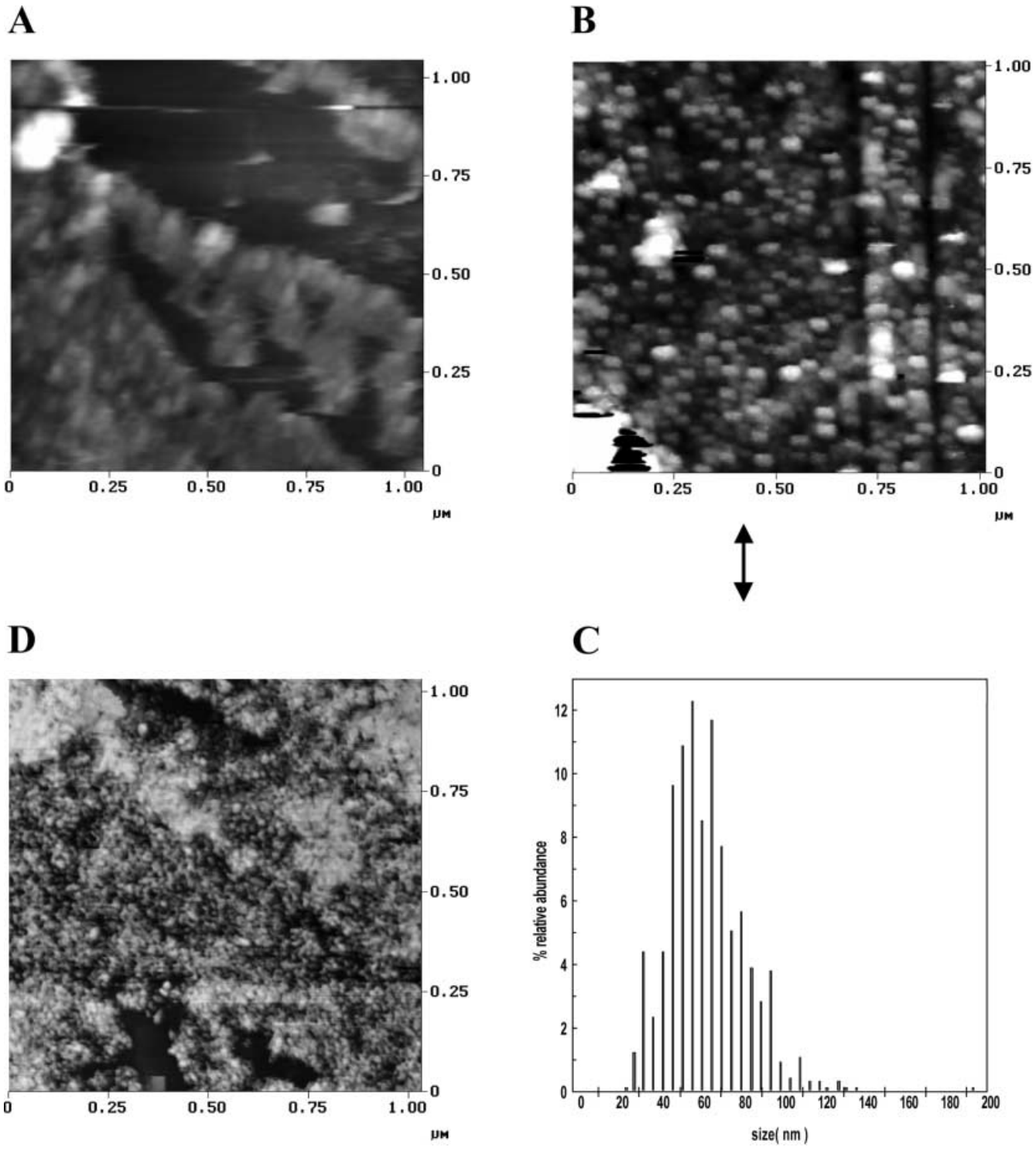

Fig. 7A–D In situ contact mode AFM images of a HOPG electrode cycled between −0.2 V and −0.87 V vs. SCE in a solution of 0.2 M Na_2SO_4 + H_2SO_4 (pH 3.50) + 10^{-4} M $[P_2Mo_{18}O_{62}]^{6-}$. **A** image acquired after 2 cycles; **B** image acquired after 6 cycles; **C** size distribution diagram of image **B**; **D** ex situ contact mode AFM image acquired after 15 cycles, with the electrode left to dry in air before imaging. Image scan rate: 1.0 Hz. No filtering was applied. For further details, see text

bath containing 10^{-4} M P_2Mo_{18} at a scan rate of 10 mV/s. We found that the deposition/modification process occurs at an appreciable rate. For instance, with one cycle and a half, the surface coverage is already significant enough for easy imaging by AFM. The statistics of size distribution on such a film indicate the presence of monomers and smaller particles, but larger particles are also detected with a preponderance of size around 21 nm. This experiment underscores the fast

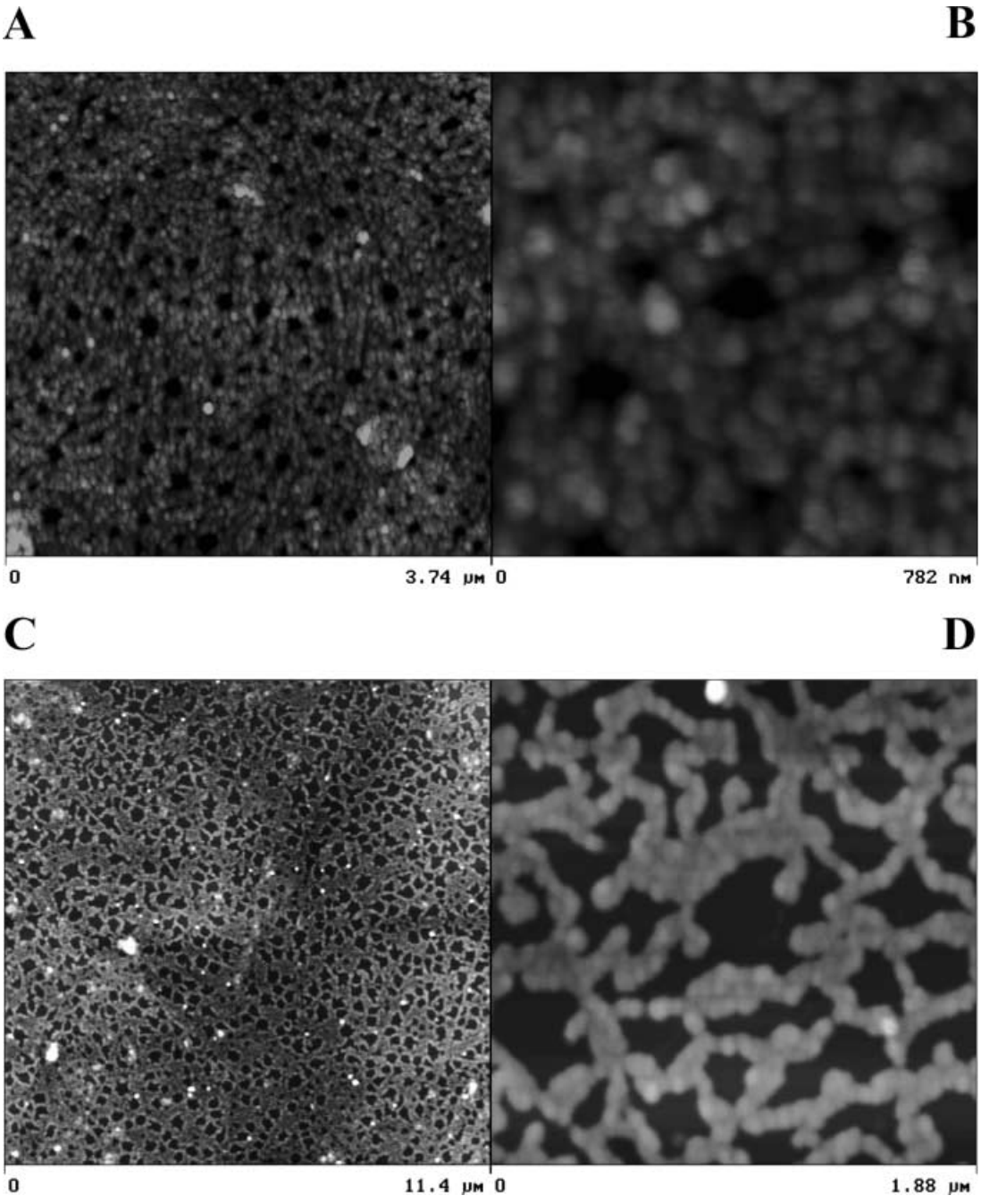

Fig. 8A–D Tapping mode AFM images in two characteristic areas of a HOPG electrode cycled between −0.2 V and −0.87 V vs. SCE during 0.5 h in a Na_2SO_4 medium (pH 4.50) + 10^{-4} M $[P_2Mo_{18}O_{62}]^{6-}$. **A**, **B** height image of a typical domain and its enlargement; **C**, **D** phase image of another typical domain and its enlargement. Image scan rate: 1.0 Hz. No filtering was applied. For further details, see text

growth of particles when the electrode remains with the heteropolyanion in the modification bath.

Then, the main observation with the present technique is that the film thickness increases fast, at least during the first several cycles. As a consequence, films are rapidly obtained which can no longer be imaged by STM. It was then necessary to shift to AFM imaging. In situ and ex situ experiments were carried out.

The pH 3.50 solution with 10^{-4} M P_2Mo_{18} was used for the in situ experiments. The cyclic voltammograms in the modification regime were run between −0.2 V and −0.87 V. In line with previous observations, the first several cyclic voltammograms are not perfectly reversible. As expected, they correspond to the build-up of a thick layer on the electrode. The contact mode AFM images acquired during the potential cycling are shown in Fig. 7. Figure 7A was captured after the second cycle, Fig. 7B after the sixth cycle. Statistics displayed in Fig. 7C show the distribution of sizes in Fig. 7B with a predominant dimension around 56 nm. As expected, the

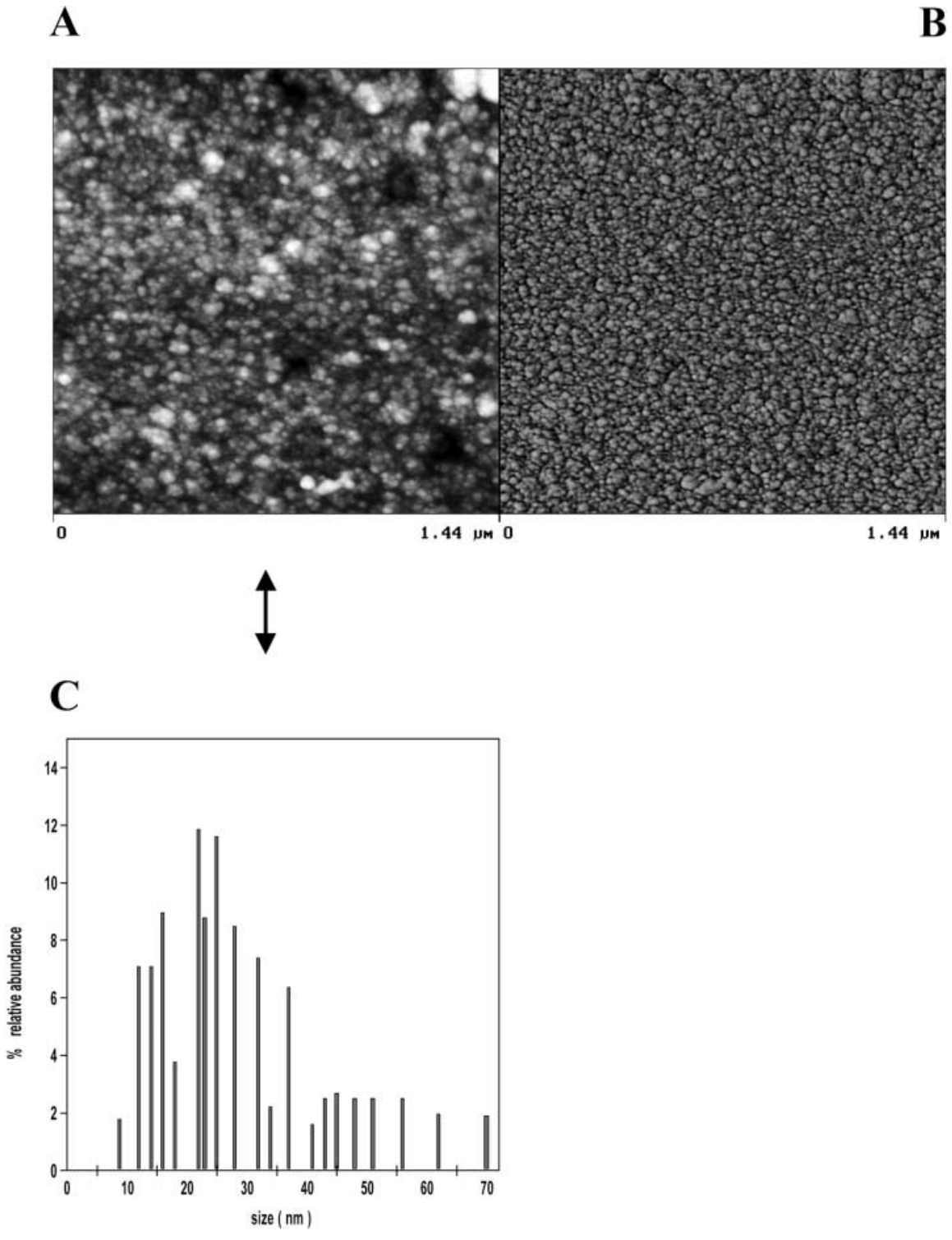

Fig. 9A–C Tapping mode AFM image of a HOPG electrode cycled between −0.2 V and −0.87 V vs. SCE during 1 h in a Na_2SO_4 medium (pH 4.50) + 10^{-4} M $[P_2Mo_{18}O_{62}]^{6-}$. **A** height image; **B** the corresponding phase image; **C** size distribution diagram established with **A**. Image scan rate: 1.0 Hz. No filtering was applied. For further details, see text

average size is larger than that observed in the preadsorption techniques, even though it remains modest, probably owing to the small number of cycles. This observation should be traced to the possibility, in the present modification method, to feed continuously new molecules from the solution into the film. Figure 7D shows an ex situ image of the electrode which was left to dry after the 15th cycle. Comparison of these three images is interesting in at least two respects. It indicates clearly the evolution from the incomplete layers with some random islands in Fig. 7A to the uniform pattern obtained in Fig. 7B. It shows also that the islands in

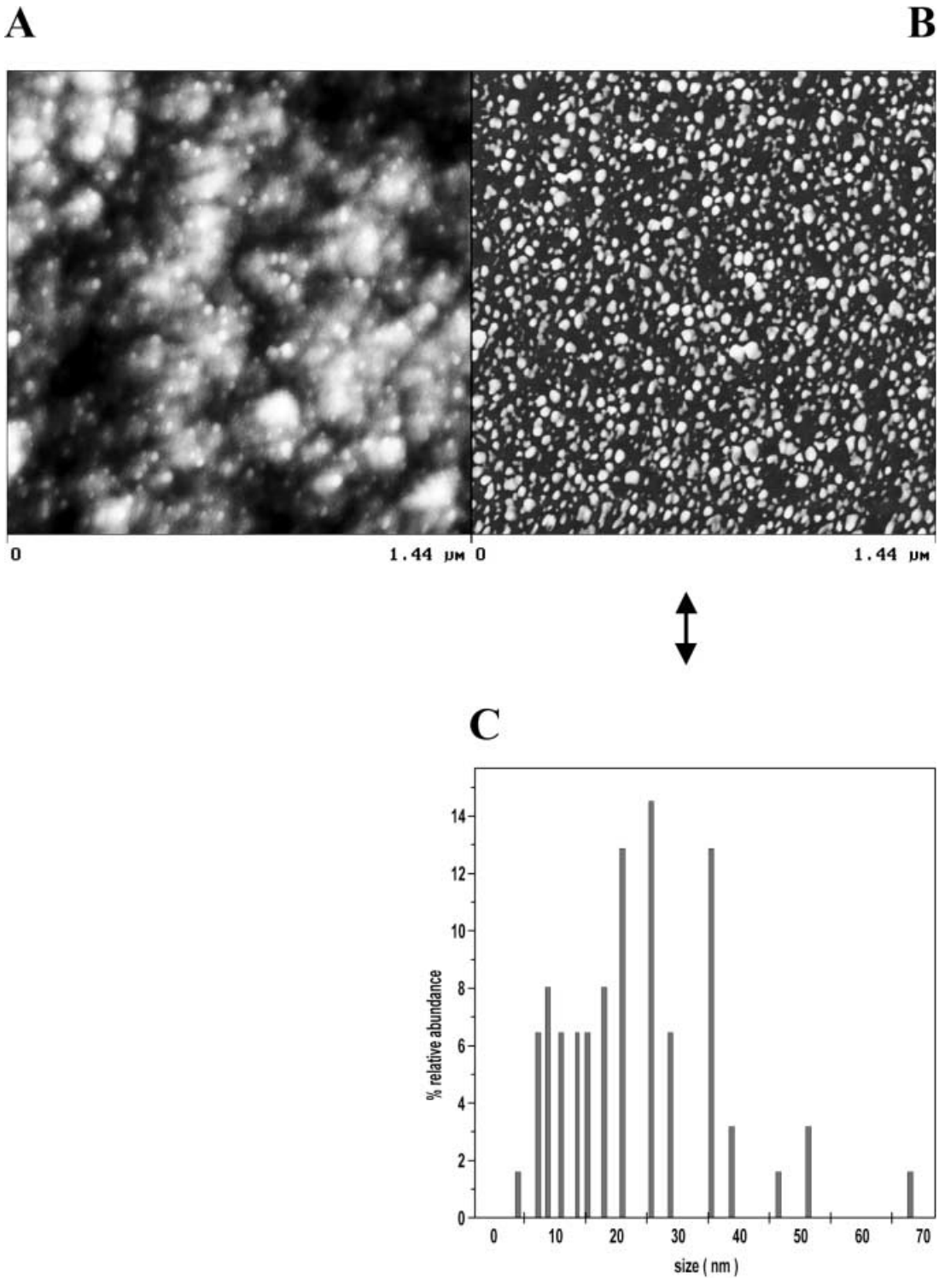

Fig. 10A–C Tapping mode AFM image of a HOPG electrode cycled between −0.2 V and −0.87 V vs. SCE during 1 h in a solution of 0.2 M $CF_3CO_2^-/CF_3CO_2H$ (pH 4.50) + 10^{-4} M $[P_2Mo_{18}O_{62}]^{6-}$. **A** height image; **B** the corresponding phase image. Image scan rate: 1.0 Hz. No filtering was applied. For further details, see text

Fig. 7D might be partly due to the drying process. As a further step in this study, it was desirable to come close to the duration conditions used in our previous experiments [6, 7]. Therefore, the cycling was continued for 0.5 h, 1 h or 3 h before stopping, rinsing and imaging. In addition, we attempted to combine the duration with the foreseeable effect of an increase of pH on the speed of film growth. This series of experiments was performed in a conventional cell and ex situ images were run.

Figure 8 was acquired in the tapping mode AFM after 0.5 h cycling in a pH 4.50 sulfate medium. The two

typical areas detected on the electrode surface are shown as representative images in Fig. 8A and C. Enlargement of both images in Fig. 8B and D, respectively, reveals the build-up of the film. Each layer is constituted by a series of interconnected small islands, typically 7–9 nm high in Fig. 8D. The objects that can be individually distinguished on the topmost layer range from 5 nm through 8 nm and up to 40 nm in diameter. Here again, as expected, these dimensions are larger than those obtained in the other modification techniques.

After 1 h cycling in the pH 4.50 sulfate medium, the main observation in Fig. 9 is a thicker patch of aggregates on the electrode surface. The size distribution of these aggregates in Fig. 9 shows that most objects remain less than 40 nm in diameter. Comparison of these results for 0.5 h and 1 h with that obtained at pH 3.50, just after one cycle and a half (ex situ experiment) or after six cycles (in situ imaging), suggests strongly that the degree of aggregation does not increase very quickly with time nor with pH. This observation induces us to investigate at least a longer cycling duration.

Figure 10, obtained with an electrode cycled for 3 h in a $CF_3CO_2^-/CF_3CO_2H$, pH 4.50, medium shows a relatively uniform coverage, but is apparently not different from the patterns in Figs. 8 and 9. In contrast to previous determinations, the statistics of size distribution in Fig. 10 were performed on the phase image which presents sharp contours for the objects on the surface. Even though this difference in the imaging modes might restrict the comparability of the data, the results for Fig. 10 tend to support the following conclusions: (1) despite the duration and the pH, the average dimensions remain predominantly smaller than 40 nm; (2) the distribution tends to become uniform over this dimension range; in other words, no single dimension seems to predominate over the others.

Here again, these observations support the conclusion that, in the present experimental conditions, the aggregation extent remains limited.

Concluding remarks

Several remarks emerge from the results of the present experiments. Despite the variety of electrode preparation techniques, the observations converge to indicate only one main difference: simple adsorption or electrochemical adsorption of the heteropolyanion prior to the modification of the electrode in pure supporting electrolyte must be contrasted with direct modification in the presence of P_2Mo_{18} in solution. In the former case, the limited amount of oxometalate confined to the electrode surface generates molecular aggregates with the most significant size in the range of 10–12 nm, while in the latter technique, the predominant dimensions reach 40 nm. The possibility for the bathing solution to contribute new molecules into the film during the modification process constitutes a simple rationale for this observation. In any case, it is remarkable that the largest dimensions observed so far in the topmost layers remain modest. Turning more specifically to the modification in pure supporting electrolyte after adsorption, it is worth noting that several monomolecular height incomplete layers have been observed, which would suggest that 3D growth of the films is possible even with a tiny amount of heteropolyanion adsorbed on the electrode surface. Furthermore, relatively large-scale AFM images show that the topmost layer films are constituted of interconnected islands. The similarity of several in situ and ex situ patterns proves that these islands do not appear solely as a consequence of drying. It thus appears that experimental conditions can be found to control, at least partly, the sizes of the agglomerates.

Further discussion is postponed until a sufficient knowledge of the average formula of the film justifies reasonable structural propositions, and hence, aggregation pathways. The problem remains a challenging one. As a matter of fact, the complexity of the electrochemical behaviour of molybdenum oxide is not completely resolved [24]. However, the case of P_2Mo_{18} can, tentatively, be paralleled with the results obtained after irradiation of ammonium molybdophosphate with a large dose of electrons [25]. This heteropolyanion was shown to be partly converted to MoO_3 and ammonium molybdate, with the eventuality for the oxide to remain coated on the original salt. In the present work, it is likely that a partial decomposition, analogous to that described above, is obtained, which might induce the main properties of the present films. Work is underway in this direction.

Acknowledgements This work was supported by the CNRS (UMR 8610 and UPRESA 7071) and by the Universities Paris XI and Paris VI.

References

1. Keita B, Nadjo L (1989) Mater Chem Phys 22: 77
2. Keita B, Nadjo L (1993) Curr Top Electrochem 2: 77
3. Toth JE, Anson FC (1989) J Am Chem Soc 111: 2444
4. Kulesza PJ, Faulkner LR (1988) J Am Chem Soc 110: 4905
5. Sadakane M, Steckhan E (1998) Chem Rev 98: 219
6. Keita B, Nadjo L, Contant R (1998) J Electroanal Chem 443: 168
7. Keita B, Abdeljalil E, Girard F, Gerschwiler S, Nadjo L, Contant R, Haut C (1999) J Solid State Electrochem 3: 446
8. Belhouari A, Keita B, Nadjo L, Contant R (1998) New J Chem 83
9. Ciabrini JP, Contant R, Fruchart JM (1983) Polyhedron 2: 1229
10. Souchay P, Contant R, Fruchart JM (1967) CR Acad Sci Paris 264: 976
11. Papaconstantinou E, Pope MT (1967) Inorg Chem 6: 1152
12. Keita B, Nadjo L (1988) J Electroanal Chem 243: 87
13. Keita B, Nadjo L, Gachard E, Remita H, Khatouri J, Belloni J (1997) New J Chem 21: 851
14. Magonov SN, Elings V, Whangbo MH (1997) Surf Sci 375: L385
15. Keita B, Nadjo L (1988) J Electroanal Chem 247: 157
16. Izumi Y, Hasebe R, Urabe R (1983) J Catal 84: 402

17. Kasztelan S, Payen E, Moffat JB (1988) J Catal 112: 320
18. Keita B, Nadjo L (1993) J Electroanal Chem 354: 295
19. Rong C, Anson FC (1994) Anal Chem 66: 3124
20. Castillo MA, Vasquez PG, Blanco MN, Caceres CV (1996) J Chem Soc Faraday Trans 92: 3239
21. Keita B, Nadjo L, Belanger D, Wilde CP, Hilaire M (1995) J Electroanal Chem 384: 155
22. Kuhn A, Anson FC (1996) Langmuir 12: 5481
23. Pope MT, Müller A (1991) Angew Chem Int Ed Engl 30: 34
24. Anbananthan N, Rao KN, Venkatevan VK (1994) J Electroanal Chem 374: 207
25. Narasimharao KL, Sarma KS, Mathew C, Jadhav AV, Shukla JP, Natarajan V, Seshagiri TK, Sali SK, Dhiwar VI, Pande B, Venkataramani B (1998) J Chem Soc Faraday Trans 94: 1641